Journal of Neuroscience Methods 209 (2012) 227–234

Contents lists available at SciVerse ScienceDirect

Journal of Neuroscience Methods

journal homepage: www.elsevier.com/locate/jneumeth

Basic Neuroscience

# Quantitative single-cell ion-channel gene expression profiling through an improved qRT-PCR technique combined with whole cell patch clamp

K. Veys[a,b], A.J. Labro[a], E. De Schutter[b,c,1], D.J. Snyders[a,*,1]

[a] Laboratory for Molecular Biophysics, Physiology and Pharmacology, Department of Biomedical Sciences, University of Antwerp, Belgium
[b] Theoretical Neurobiology, Department of Biomedical Sciences, University of Antwerp, Belgium
[c] Computational Neuroscience Unit, Okinawa Institute of Science and Technology, Japan

ARTICLE INFO

*Article history:*
Received 17 February 2012
Received in revised form 17 May 2012
Accepted 9 June 2012

*Keywords:*
RNA amplification
Shaker-type ion channel
Kv2.1
Quantifying transcripts
Embryonic dorsal root ganglion neurons

ABSTRACT

Cellular excitability originates from a concerted action of different ion channels. The genomic diversity of ion channels (over 100 different genes) underlies the functional diversity of neurons in the central nervous system (CNS) and even within a specific type of neurons large differences in channel expression have been observed. Patch-clamp is a powerful technique to study the electrophysiology of excitability at the single cell level, allowing exploration of cell-to-cell variability. Only a few attempts have been made to link electrophysiological profiling to mRNA transcript levels and most suffered from experimental noise precluding conclusive quantitative correlations. Here we describe a refinement to the technique that combines patch-clamp analysis with quantitative real-time (qRT) PCR at the single cell level. Hereto the expression of a housekeeping gene was used to normalize for cell-to-cell variability in mRNA isolation and the subsequent processing steps for performing qRT-PCR. However, the mRNA yield from a single cell was insufficient for performing a valid qRT-PCR assay; this was resolved by including a RNA amplification step. The technique was validated on a stable Ltk$^-$ cell line expressing the Kv2.1 channel and on embryonic dorsal root ganglion (DRG) cells probing for the expression of Kv2.1. Current density and transcript quantity displayed a clear correlation when the qRT-PCR assay was done in twofold and the data normalized to the transcript level of the housekeeping gene GAPD. Without this normalization no significant correlation was obtained. This improved technique should prove very valuable for studying the molecular background of diversity in cellular excitability.



## 1. Introduction

Ion channels create gated transmembrane pores with unique gating kinetics that underlie cellular excitability (Hille, 2001). Each channel is composed of pore forming α-subunit(s) that can associate with other auxiliary subunits, which can modulate channel function or anchor the protein to cytoskeletal elements creating multi-subunit channel complexes. More than 100 different genes of α-subunits have been characterized (Catterall et al., 2005; Clapham et al., 2005; Gutman et al., 2005; Hofmann et al., 2005; Wei et al., 2005), which are further diversified by alternative splicing and post-translational modifications. This results in a wide variety of in vivo currents, presumably subserving the specific need of the various excitable tissues.

Obviously, this diversity complicates the characterization of the underlying molecular architecture of the channel complex (Fig. 1A). Even among neurons of a same type, large differences in the level of channel expression have been observed (Achard and De Schutter, 2006; Aptowicz et al., 2004; Mee et al., 2004; Schulz et al., 2006; Swensen and Bean, 2005). Furthermore, during development the expression profile of channel subunits may change substantially (Butler et al., 1998; Fitzakerley et al., 2000; Franco et al., 2001). The patch-clamp technique, a technique used to study the electrophysiology of excitable cells (Hamill et al., 1981), operates at the single cell level and allows exploration of cell-to-cell phenotypic variability. This variability can be the result of different mRNA transcript levels or originate from differences in post-translational modification such as e.g. phosphorylation. Therefore, analyzing both the transcriptome and the electrophysiological profile of the same cell could prove whether the observed variability finds its origin in the mRNA pool or not.

Most studies have combined patch-clamp experiments with end-point PCR and simplified variability to the presence or absence of expression (Audinat et al., 1996; Bochet et al., 1994; Chiang, 1998; Koizumi et al., 2004; Lambolez et al., 1992; Nissant et al.,

* Corresponding author at: Department of Biomedical Sciences, University of Antwerp (UA), Universiteitsplein 1, 2610 Antwerp, Belgium. Tel.: +32 3 265 23 35; fax: +32 3 265 23 26.
*E-mail address:* dirk.snyders@ua.ac.be (D.J. Snyders).
[1] These authors contributed equally to this work.

0165-0270/$ – see front matter © 2012 Elsevier B.V. All rights reserved.
http://dx.doi.org/10.1016/j.jneumeth.2012.06.008

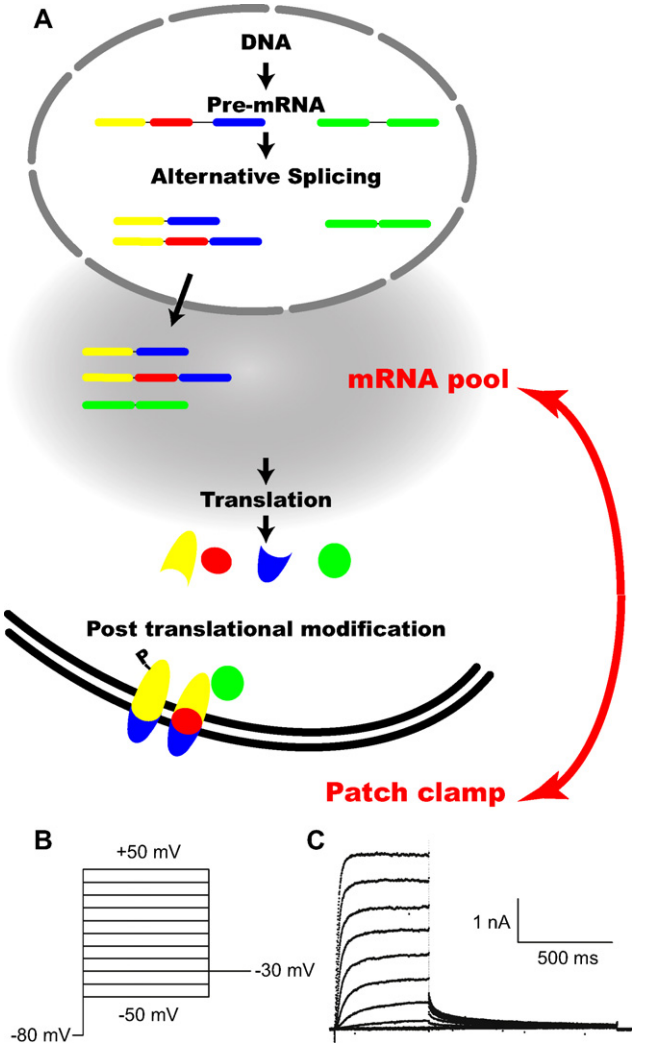


**Fig. 1.** (A) Overview of molecular processes leading to diversity in biophysical properties of voltage gated channels. These channels are composed of multiple subunits that show lots of diversity because they originate from multiple genes undergoing splicing in the nucleus. Also posttranslational modifications (for example phosphorylation) further increase diversity. (B) Voltage clamp protocol for Kv2.1 using 500 ms step protocol ranging from −50 to +50 mV in 10 mV steps. (C) Example of Kv2.1 currents in Ltk⁻ cells.

2004; Toledo-Rodriguez et al., 2004). A few attempts have been made to combine single cell patch clamping with quantitative techniques measuring mRNA of the same cell, but they suffered from experimental noise making correlations between the electrophysiological data and mRNA transcript levels very difficult (Liss et al., 2001). This noise has multiple possible sources: variable extraction efficiency, differences in reverse transcription efficiency and the quantification by real-time PCR itself. Here we describe a refinement and optimization of the technique that combines whole cell path clamp analysis with quantitative real-time (qRT) PCR to determine the amount of a specific transcript at the single cell level. We applied it to the expression of Kv2.1 channels, a type of delayed rectifier potassium channel that regulates action potential duration and neuronal excitability (Blaine and Ribera, 1998; Misonou et al., 2005). In both stably transfected mouse Ltk⁻ cells expressing Kv2.1 and mouse embryonic dorsal root ganglion neurons a good correlation between delayed rectifier current density and Kv2.1 transcript level was obtained, after proper normalization.

## 2. Materials and methods

### 2.1. Electrophysiology

RNAse free patch pipettes were made from borosilicate glass capillaries with an outer diameter of 1.5 mm (Hilgenberg, Malsfeld, Germany) by baking the glass capillaries for at least 2 h at 200 °C after sonication in absolute alcohol. Pipettes with a resistance ranging from 2 to 4 MΩ were pulled on a horizontal P-87 puller (Sutter Instrument company, Novato, USA). Electrophysiological recordings were done at room temperature (21–23 °C) with an Alembic VE-2 Voltage clamp amplifier (Alembic Instruments Inc., Montreal, Canada) in the whole cell configuration and pulse protocols were controlled using pClamp 10 software (Axon Instruments, Union City, CA). Ltk⁻ cells and DRG neurons were clamped at −80 mV and 500 ms or 250 ms depolarizing steps were applied to potentials from −50 mV to +50 mV in 10 mV increments (Fig. 1B and C). In case of DRG neurons the 250 ms depolarizing step protocol was repeated after 3 min with the perfusion of 100 nM sStromatoxin-1 (ScTx) (Alomone Labs, Jerusalem, Israel). Kv2.1 currents were measured by subtracting the peak current before and after application of ScTx at +10 mV at which the block of ScTx is maximal and voltage clamp was optimal (Bocksteins et al., 2009). Current recordings were filtered with a 10 kHz low-pass Bessel filter and digitized with an Axon digidata board 1322A series at 25 kHz. Series resistance was compensated up to 95% and ranged from 4.4 to 7.3 MΩ for Ltk⁻ cells and from 3.3 to 5.6 MΩ for DRG neurons before compensation. Membrane capacitance, access, and seal resistance were determined using repetitive square voltage-command pulses. Cells were continuously superfused with extracellular solution made (ECS) from RNAse free chemicals and ultra-pure water (Merck Millipore, Bellerica, MA, USA) containing for Ltk⁻ cells (in mM): 145 NaCl, 4 KCl, 1 $MgCl_2$, 1.8 $CaCl_2$, 10 HEPES, 10 glucose and adjusted to pH 7.35 with NaOH. ECS for DRG neurons: 140 NMG, 5 KCl, 1 $MgCl_2$, 1.8 $CaCl_2$, 5 HEPES, 10 glucose and adjusted to pH 7.4 with NaOH, osmolarity adjusted to 315 mOsm with sucrose. Intracellular solution (ICS) was made from ultra-pure DNAse and RNAse free water (Invitrogen, Carlsbad, CA, USA) containing for Ltk⁻ cells (in mM) 110 KCl, 5 $K_2ATP$, 2 $MgCl_2$, 10 HEPES, $K_4BAPTA$ with the pH adjusted to 7.2 using KOH. ICS for DRG neurons: 6 NaCl, 110 K-gluconate, 20 KCl, 2 $Na_2ATP$, 2 $MgCl_2$, 10 HEPES, 2 EGTA, 2 $MgCl_2$, 1 $CaCl_2$, pH adjusted to 7.4, osmolarity adjusted to 306 mOsm with sucrose.

### 2.2. Cell culture

The stably transfected mouse Ltk⁻ cells containing the pMSV-Neo vector with human Kv2.1 was created as described previously (Snyders et al., 1993). The vector contained a dexamethasone-inducible murine mammary tumor virus promoter controlling transcription of Kv2.1. Cells were cultured in DMEM (Invitrogen) supplemented with 10% horse serum (Invitrogen), 1% penicillin/streptomycin and 0.25 mg/ml G418 (Invitrogen) under a 5% CO2 atmosphere. 16 to 24 h after promoter induction with 2 μM dexamethasone (Sigma–Aldrich, St Louis, MO, USA) the cells were harvested by trypsinization and used for analysis within 12 h. Embryonic dorsal root ganglion cultures were prepared as previously described (Bocksteins et al., 2009).

### 2.3. Molecular biology

#### 2.3.1. Reverse transcription

Under visual control, the content of the patch clamp pipette (1 μl) that contained the mRNA of the cell was expelled in a 0.2 ml thermo tube (Westburg, Leusden, Netherlands) containing 1 μl of premixture solution, which was made the same day and kept at

−20 °C until use. The premixture contained 1 ng of MluT7 primer (Moll et al., 2004), 4 units of RnaseOUT (Invitrogen) 0.5 μg T4gP32 (USB, Cleveland, OH, USA) and 2 mM dNTP (Invitrogen). After adding the cell content to the premixture everything was immediately flash frozen in liquid nitrogen. The combination of cooling and ribonuclease inhibitors prevented RNA breakdown before further processing of the sample.

Before the reverse transcription (RT) reaction the RNA-premixture sample was denaturated for 2 min at 70 °C. For the RT we used a 5 μl reaction volume composed of 1 μl premixture solution, 1 μl cell mRNA and 3 μl of RT mixture that contained 5 units sensiscript (Qiagen, Hilden, Germany) with its corresponding buffer, 20 units of Superscript III (Invitrogen) and 10 units of RNaseOUT (Invitrogen). The RT reaction proceeded as follows: 20 min at 37 °C, 42 °C and 50 °C each, 10 min at 60 °C and finally 15 min at 70 °C to stop the reaction. The Poly-T primer used in the RT reaction, named MLuT7 had a one nucleotide anchor at its 3′ and a full T7 promotor at its 5′ end (Moll et al., 2004) for subsequent antisense RNA amplification. This primer was 64 nucleotides long with sequence: 5′-GGAGGCCGGAGAATTGTAATACGACTCACTATAGGGACGCGTGTTT-TTTTTTTTTTTTTTTTV-3′ where V represents a random nucleotide A, G or C. After the RT reaction the remaining RNA strand was degraded with 1 unit RNAse E (Invitrogen) and a 5′ poly A-tail was created simultaneously with 3 units terminal deoxynucleotidyl transferase (Invitrogen) using 1.12 mM ATP (Promega, Madison, WI, USA) in a 15 μl reaction volume. This allowed full-length synthesis of the second strand with 0.5 units of platinum Taq high fidelity DNA polymerase (Invitrogen) on a temperature gradient: 1 min at 94 °C, 10 min at 40 °C and 50 min at 68 °C using a conventional poly-T primer (1 ng) in a 25 μl reaction volume. After second strand synthesis, all enzymes were removed by 80 μl chloroform/phenol extraction using heavy phase lock gels (5 prime, Hamburg, Germany).

#### 2.3.2. RNA amplification/in vitro RNA synthesis

The cDNA was precipitated to change buffers and to remove all free dNTPs (<20 bp). This was done by aliquoting the cDNA from around 10 to 36 μl with TE-buffer (Invitrogen) and mixing thoroughly with 5 μg linear poly-acrylamide (GenElute-LPA, Sigma), 4 μl 3 M sodium acetate solution adjusted to pH 5.2 with glacial acetic acid, and 100 μl absolute (99.9%) ethanol (Gaillard and Strauss, 1990). The pellet was spun down at 13,000 rpm for 30 min at 4 °C and washed with 70% ethanol and this 3 times.

The pellet was dissolved in the premix of the in vitro RNA transcription reaction: 20 units/μl T7 polymerase and buffer (Promega), 200 mM rNTPs (Promega), 80 units RNaseOut (Invitrogen), 200 mM DTT (Promega). Amplification was done in a thermal cycler (Biometra, Goettingen, Germany) at 37 °C for 8 h in a 20 μl reaction volume. The amplified RNA was filtered on a Microcon-100 filter (Milipore), first with TE buffer (250 μl) and then with $ddH_2O$ (250 μl). The amplified RNA was subsequently reverse transcribed using the similar temperature sequence as that of the first RT but the reaction volume was increased to 30 μl containing 40 units RNaseOUT, 5 mM dNTP, 2 μg T4 Gene 32 protein, 10 units Sensiscript, 100 units Superscript III, 0.15 μM Poly-T primer and 25 ng random hexamers (Invitrogen). cDNA was made by first degrading the mRNA transcripts with 0.5 units of *E. coli* RNAse H (Invitrogen) in a 30 μl reaction volume followed by second strand synthesis with 0.5 units of Platinum High Fidelity Taq polymerase (Invitrogen) in 40 μl reaction volume. The product was cleaned as detailed above with chloroform/phenol using a phase lock gel and precipitated with 1 μl linear polyacrylamide, 10 μl sodium acetate and 200 μl ethanol. The pellet was cleaned with 160 μl 70% ethanol and dissolved in 14 μl ddH2O (the appropriate volume for 4 qRT-PCR assays of 3 μl each + 2 μl residual volume).

#### 2.3.3. Quantitative real-time (qRT) PCR

qRT-PCR was performed on a Lightcycler 480 (Roche, Basel, Switzerland) using Roche master mix probes in a 12 μl reaction volume. Primers for GAPD were custom designed and obtained from Eurogentec (Liège, Belgium): TTCACCACCATGGAGAAGGC (sense), GGCATGGACTGTGGTCATGA (antisense) and TGCATCCTG-CACCACCAACTGCTTAG (probe) based on its reference sequence NM_008084.2. Kv2.1 primers/probe for $Ltk^-$ cells were purchased from Applied Biosystem (Invitrogen). Primers/probe for DRG neurons were custom designed and obtained from Eurogentec: AAGAAACTTTGGGACCTGCT (sense), GAATTCGTCCAGGCTCTGTAG (antisense) and CCACCGATGAGTTGGGCTTCTCC (probe) based on its reference sequence NM_008420. Cycle threshold ($C_t$) levels were rescaled by their average and transformed into relative quantities (RQ) using the amplification efficiency as described by Pfaffl (2001). The normalized relative quantity (NRQ) of Kv2.1 was calculated by dividing the RQ by the normalizing factor (NF) using the following formula $NRQ_{jk} = RQ_{jk}/NF_k$ (Vandesompele et al., 2002). If only one housekeeping gene is used the NF equals the RQ of that housekeeping gene; if multiple genes are used it equals the geometric mean of their RQs.

## 3. Results

### 3.1. Whole cell patch clamp in combination with qRT-PCR

The RNA content of a single neuron is extremely low. On average a vertebrate neuron contains 50 pg of total RNA, 2% of which is mRNA. For a specific ion channel amounts of 0.2–2 fg of mRNA have been estimated, corresponding to a few tens to a few hundreds of actual molecules (Sucher et al., 2000). Consequently the cDNA yield (after reverse transcription of the isolated mRNA, see Section 2.3.1) is not sufficient to adhere to the general guidelines for performing qRT-PCR (Derveaux et al., 2010), which state the need for normalization to reduce technical noise. This relative quantification strategy implies analyzing at least one housekeeping gene together with the gene(s) of interest and both assays done in twofold, preferentially threefold. By optimizing the mRNA processing steps and the introduction of an RNA amplification step we managed to obtain adequate cDNA yields in order to meet these qRT-PCR guidelines (Derveaux et al., 2010) and show a significant reduction in inherent experimental noise.

mRNA was extracted via the patch clamp pipette by dialysis of the cell and by applying negative pressure in the pipette at the end of the electrophysiological recordings, which lasted at least 15 min (Ohya and Sperelakis, 1988). Permanent visual control ensured that there was no contamination by other cells and that the nucleus was not extracted. This eliminated the need for a DNAse step during mRNA processing which is an advantage since heat inactivation of DNAse has been shown to facilitate chemically induced scission of RNA (according to manufacturer's guidelines, Ambion). The effective extracted amount depended on the pipette shape, the access resistance to the cell and the duration of the experiment. Variations of these parameters are inherent to the technique of "whole cell" patch-clamp. The electrophysiological recordings and the mRNA extraction procedure were performed at room temperature. To minimize the mRNA degradation during this procedure, all solutions, electrodes, pipettes and perfusion system were treated to be RNAse free (see Section 2).

The subsequent reverse transcription (RT) is the second largest source of experimental variability after sample collection (Stahlberg et al., 2004) and was therefore optimized (Fig. 2). The

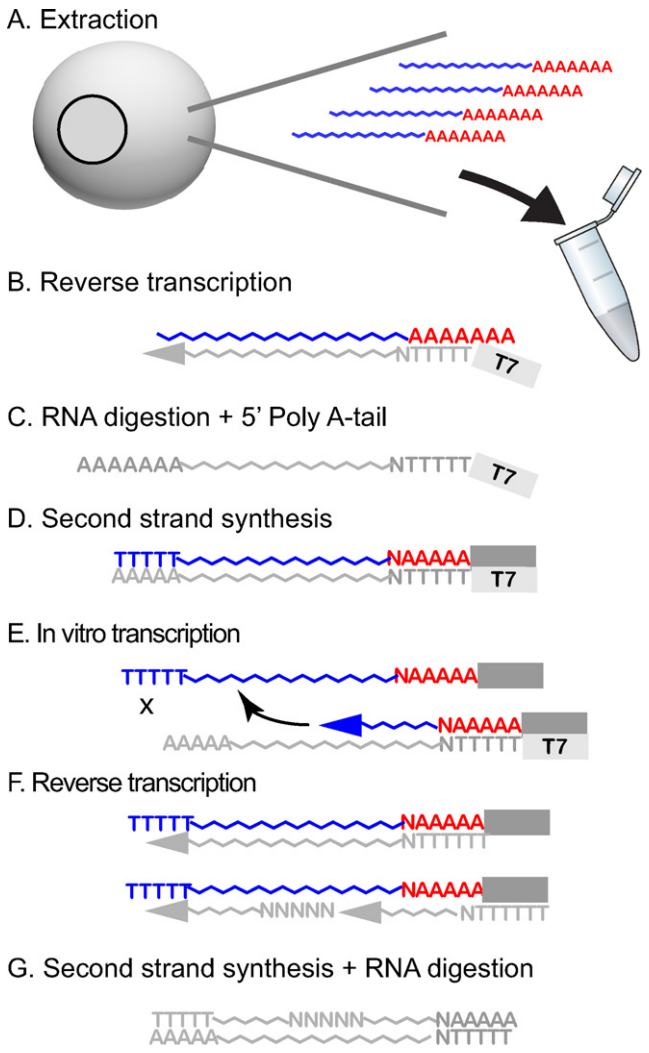


**Fig. 2.** Overview of molecular procedures from mRNA extraction to amplified cDNA. (A) Extraction of mRNA via diffusion from the soma to the patch pipette and extraction in a tube. (B) Reverse transcription with anchored poly-T primer containing T7 promoter. (C) Degradation of RNA strand and addition of Poly-A tail. (D) Second strand synthesis. (E) 8 h in vitro RNA synthesis. (F) Reverse transcription using both poly-T and random primers. (G) Second strand synthesis after RNA digestion.

reaction was scaled down to 5 μl, since the efficiency of the RT reaction depends not only on the total amount of target RNA but also on the RNA concentration (Karrer et al., 1995; Stahlberg et al., 2004). Decreasing the RT reaction volume further was not possible due to the ATP concentration from the intracellular recording solution (ICS). ATP is a usual and necessary component of the ICS. Furthermore, the patch-clamp technique itself puts a physical limit of 1 μl ICS within the pipette for having a stable contact with the electrode. RT was designed to obtain full-length cDNA since most channel transcripts show a high degree of homology or have multiple splice variants. Therefore, the reaction was primed with an anchored poly-T sequence extended with a T7 promoter MLuT7 (Moll et al., 2004) (Section 2.3.1). The anchor ensured that the reaction was initiated on the 5′ end of the poly-A tail from the mRNA strands, because long stretches of poly-A could stall the enzyme, and reduced internal priming in poly-A stretches within the mRNA (Nam et al., 2002). The concentration of primer was scaled down from the conventional 1 μM (manufacturer's guidelines, Qiagen) to 10 nM because the concentration of mRNA was still 200–2000 times lower than in conventional reactions and excess of poly-T primer could favor internal priming (Nam et al., 2002). Lowering the primer concentration was also beneficial for the RNA amplification at a later stage in the process since the primer then could form dimers that might serve as a template for the polymerase reaction, thereby lowering the RNA amplification efficiency. For the RT reaction a combination of two different enzymes was chosen: sensiscript (Bosch et al., 2000), to ensure optimal priming of the poly-A tail at 37 °C, and superscript, because it is active at higher temperatures and the reaction conditions were increased up to 60 °C for dealing with secondary RNA structures and GC rich sequences (Stone et al., 1995).

The subsequent second strand synthesis reaction was done in a 25 μl volume to dilute the RT enzymes a 5-fold such that their inhibiting effect on Taq polymerase activity was lowered (Sellner et al., 1992). Although inactivated by heat, RT enzymes could still bind the DNA and severely affect Taq activity, especially when working with small concentrations as in single cells (Chandler et al., 1998). Adding T4 gene 32, a single strand binding protein that is presumed to stabilize the DNA or displace RT enzymes from the template (Chandler et al., 1998; Topal and Sinha, 1983; Williams et al., 1981), further increased the efficiency of the Taq enzyme. Full-length second strand synthesis was achieved as described in Section 2.3.1.

To obtain enough material to meet the guidelines for qRT-PCR a RNA amplification step was introduced. Prior to the RNA amplification, the cDNA was cleaned first by chloroform extraction to remove all enzymes and followed by precipitation to remove nucleotides. The method chosen for precipitation was using linear polyacrylamide, which has a complete recovery of fragments larger than 20 bp, thereby removing all unincorporated primers and nucleotides (Gaillard and Strauss, 1990) as necessary for the subsequent mRNA amplification step (Section 2.3.2). The amplified mRNA was converted to double stranded cDNA using similar procedures as described above but compared to the single cell mRNA RT reaction the reaction volumes and reagent concentrations were increased to meet the amplified amount of mRNA (Section 2.3.2).

### *3.2. Validation of the technique: direct single cell correlation between Kv2.1 current density and transcript level*

To validate our technique we used a Ltk$^-$ cell line that stably expresses Kv2.1 channels under control of an inducible promoter. Maximal induction of expression by dexamethasone yielded currents in the range of 1–5 nA (Fig. 2), which represents a reasonable density suited for voltage clamp analysis without problems of series resistance errors. The channel expression was not saturated in this stable Ltk$^-$ cell line since transient transfection easily resulted in cells expressing 10 times more current (data not shown). Cell-to-cell variation in current density can be attributed to randomness at multiple levels: intrinsic variation due to the stochastic nature of promoter activation which is a typical feature of the process (Ansel et al., 2008; Mitarai et al., 2008) and extrinsic factors (Swain et al., 2002) such as the state in the cell cycle and the actual amount of dexamethasone uptake. This model system was therefore very well suited to validate the technique as a test for analyzing cell-to-cell variability in gene expression, which was reflected by the measured current density.

To calculate the relative quantity (RQ) from the obtained $C_t$ values, the PCR efficiency needs to be known for each of the genes tested. The PCR efficiencies were determined by using a series of 10-fold dilutions from whole brain cDNA (Fig. 3A). The efficiency of the assays, calculated by linear regression, was $1.83 \pm 0.16$ ($n = 3$) for the housekeeping gene glyceraldehyde 3-phosphate dehydrogenase (GAPD) and $1.94 \pm 0.35$ ($n = 3$) for Kv2.1 (Fig. 3, panels B and C, respectively). For GAPD we observed that a 1000-fold dilution resulted in a clear reduction in efficiency. One assay had a $C_t$ level of 39.17, which was one cycle below the predicted value of the

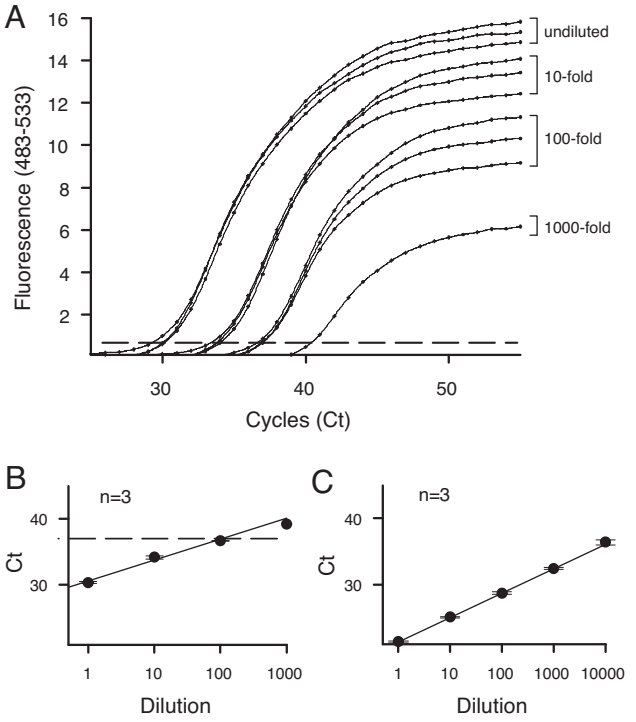


**Fig. 3.** Efficiency of the qRT-PCR assays. (A) Raw data of GAPD qRT-PCR assays showing exponential increase in fluorescence plotted against PCR cycles. 10-Fold dilutions of whole brain cDNA were used and for every dilution the assays were done in 3-fold (triplicate reactions). Note that for the 1000-fold dilution only one out of three assays worked. Dashed line represents the fluorescence threshold used to determine $C_t$ levels. (B) and (C) Standard curve for GAPD (B) and Kv2.1 (C) obtained by plotting the mean $C_t$ value ± standard deviation (obtained from the triplicate reaction, $n = 3$) as a function of the 10-fold dilution steps. Solid lines represent the linear regression with a slope 1.83 for GAPD and 1.49 for Kv2.1. The dashed line in panel (B) shows the maximum reliable $C_t$ level for GAPD (38 cycles).

linear regression and the two remaining assays failed. Therefore, the maximum useable $C_t$ level for GAPD was set to 38.

Kv2.1 expressing Ltk⁻ cells ($n = 21$) were analyzed individually and the qRT-PCR reactions were done in twofold for both Kv2.1 and GAPD with a maximum allowed difference between both replicate assays set to 0.5 cycles. This allowed to detect abnormal efficiencies or variability in the qRT-PCR reactions. Using these criteria 10 out of the 21 cells needed to be discarded: 3 cells had $C_t$ values for GAPD that were above the threshold of 38 cycles and the other 7 showed a difference of more than 0.5 cycle between the replicate assays of either GAPD or Kv2.1. It was clear that to adhere to the general guidelines for qRT-PCR (Bustin et al., 2009) it was impossible to implement the technique on single cell cDNA without RNA pre-amplification.

Housekeeping genes are known to potentially correlate with the size of cells (Silbert et al., 2003) although GAPD has been shown to be one of the most stable housekeeping genes (Vandesompele et al., 2002). A trend between the relative expression of GAPD and the cell capacitance (reflecting the cell size) was apparent, but the correlation was not statistically significant (linear regression: $r^2 = 0.02$ with $p = 0.71$) (Fig. 4A). However, the data showed a large coefficient of variation of 43%, which was presumably attributable to cell-to-cell differences in the efficiency of mRNA extraction, RT efficiency and RNA amplification.

Kv2.1 current amplitudes obtained at +50 mV, a sufficiently strong depolarizing potential to have full channel activation (Bocksteins et al., 2009) (Blaine and Ribera, 1998), showed no correlation with the measured cell capacitance (linear regression: $r^2 = 0.06$ with $p = 0.46$) (Fig. 4B). Similarly, the normalized relative quantity (NRQ) of Kv2.1 mRNA showed no significant correlation with capacitance ($r^2 = 0.40$ with $p = 0.31$) (Fig. 4C). Unexpectedly, the RQ of Kv2.1 mRNA transcripts did not show a significant correlation with the Kv2.1 current density obtained by normalizing the current amplitude to the cell capacitance (linear regression: $R^2 = 0.32$, $p = 0.07$; slope 0.189; Pearson correlation with $R = 0.54$ and $p = 0.08$) (Fig. 4D). Although a larger data set could have resulted

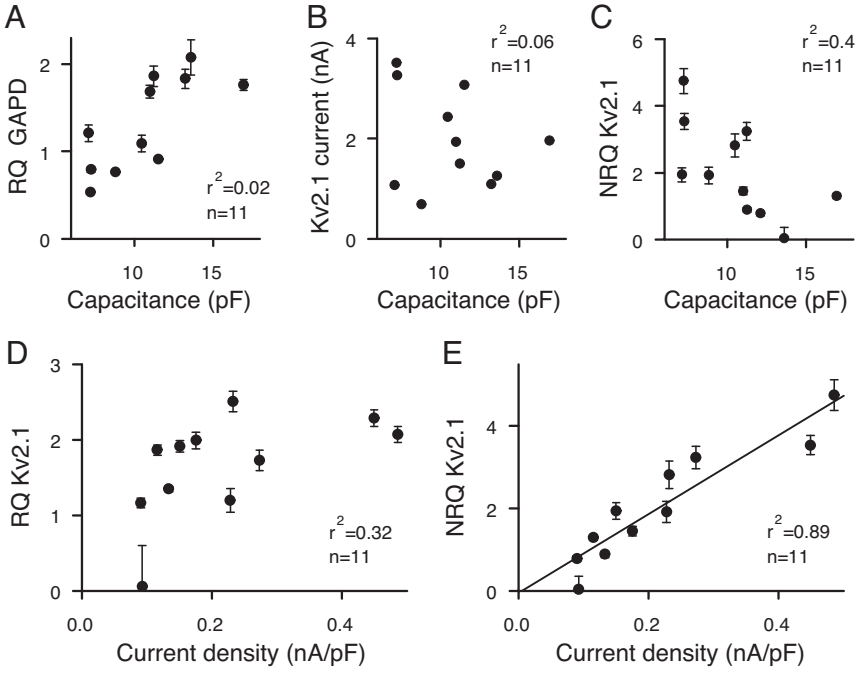


**Fig. 4.** Correlation of Kv2.1 expression and current density in Ltk⁻ cells. (A) Relative expression (RQ) of GAPD plotted against cell capacitance. (B) Peak current of Kv2.1 at +50 mV plotted against cell capacitance. (C) Normalized relative expression (NRQ) of Kv2.1 plotted against cell capacitance (D) Relative expression (RQ) of Kv2.1 plotted against the peak current normalized by cell capacitance (current density). (E) NRQ of Kv2.1 plotted against the current density. Solid line represents the linear regression ($r^2 = 0.889$).

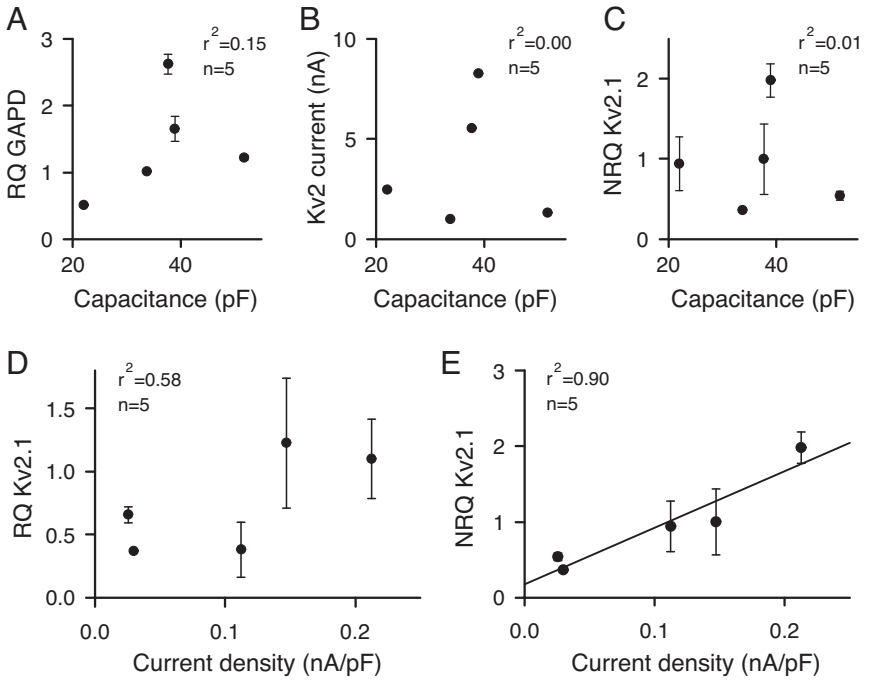


**Fig. 5.** Correlation of Kv2.1 expression and ScTx sensitive current in DRG neurons. (A) Relative expression of GAPD plotted against cell capacitance. (B) Kv2 (ScTX sensitive) current at +10 mV plotted against cell capacitance. (C) NRQ of Kv2.1 plotted against cell capacitance. (D) RQ of Kv2.1 plotted against the Kv2 (ScTx sensitive) current density. (E) NRQ of Kv2.1 plotted against the Kv2 current density.

in a more significant correlation, we hypothesized that it was variability in mRNA extraction that seriously affected the measurements. Therefore, the housekeeping gene GAPD was used as an internal control to normalize the RQ of Kv2.1. After this normalization a clearly significant correlation between the NRQ and the current density of Kv2.1 was obtained for the same set of cells (linear regression: $R^2 = 0.89$ with $p < 0.001$ and slope 0.250; Pearson correlation with $R = 0.93$ and $p < 0.0001$) (Fig. 4E).

### 3.3. Analyzing Kv2.1 expression in native embryonic DRG neurons

Ltk⁻ cells were well suited for validating the technique since there is no post-transcriptional regulation disrupting the correlation between mRNA and channel proteins. The observed variance in current density should therefore originate from the Kv2.1 transcript level. However, the goal is to analyze native expression in neurons where the amount of transcription or efficiency of translation may be different. To ensure that the technique was sensitive enough to detect a possible smaller mRNA content in neurons we conducted the same experiments on cultured mouse embryonic DRG neurons. From the ScTx sensitive current in these mouse embryonic DRG neurons, it was estimated that the majority (60–70%) of the delayed rectifier $K^+$ current is carried by Kv2 channels (Bocksteins et al., 2009).

In total 11 DRG neurons were analyzed and 5 of them passed the above-discussed criteria. Neither the housekeeping gene GAPD ($R^2 = 0.15$, $p = 0.52$), nor the raw Kv2 current amplitude that was estimated from the ScTX sensitive current ($R^2 = 0.00$, $p = 0.98$), nor the normalized expression of Kv2.1 mRNA ($R^2 = 0.01$, $p = 0.91$) showed a significant correlation with the capacitance of the cells (Fig. 5A–C, respectively). Similar as in Ltk⁻ cells, RQ of Kv2.1 mRNA transcripts did not show a significant correlation with the Kv2 current density ($R^2 = 0.58$, $p = 0.14$) (Fig. 5D). However, normalizing the relative quantity (NRQ) to the housekeeping gene GAPD again improved the quality of the regression, with a strong correlation for only 5 data points ($R^2 = 0.90$ with $p = 0.01$) (Fig. 5E).

## 4. Discussion and conclusion

Using an optimized technique that combines whole cell patch-clamp recording with qRT-PCR we obtained a significant correlation between the NRQ of Kv2.1 and its current density using the phenotypic noise of an inducible promoter in Ltk⁻ cells. Furthermore, implementing the same approach on embryonic DRG neurons yielded a strong correlation between Kv2 (ScTx sensitive delayed rectifier) current density and Kv2.1 mRNA expression level for only a limited data set. However, these correlations were only observed with the normalized (NRQ) values, i.e. after the RQ of Kv2.1 was normalized to the RQ of the housekeeping gene GAPD. The RQ of GAPD itself showed a high coefficient of variation, which was not a priori expected as it was selected for its stability within the population (Vandesompele et al., 2002). This variance was therefore attributed to inherent experimental noise or variability and was also expected to be present in the RQ of Kv2.1, since both datasets were obtained simultaneously. One of the major sources of experimental noise derives from the mRNA extraction method, which relies on the patch-clamp technique. The mRNA of the cell is transferred to the pipette by diffusion, with an efficiency that depends on pipette resistance and shape, the actual access resistance during the experiment, duration of electrophysiological recordings, aspiration at he end of the experiment, etc. This variation in efficiency between experiments will be directly reflected in the quantification of both genes. Previously, the experimental work by Liss et al. (2001) showed similar variance on the control experiments of the housekeeping gene beta-actin. These experiments relied on absolute quantification of the genes of interest because it was only possible to conduct one qRT-PCR assay per cell. The latter precluded normalization of the data that, as we show here, is essential to reduce experimental noise. Instead of using a house-keeping gene Aponte et al. (2006) compared the relative abundance of 2 transcripts expressed in the same cells. Since both transcripts were extracted and reversed transcribed in the same procedure they should be subject to the same sources of experimental variability.

Therefore, the noise originating from variability in extraction will be reduced in the calculation of the relative abundance (similar as after normalizing with a housekeeping gene).

However, because of the very low cDNA yield Aponte et al. also faced the problem of high $C_t$ levels (above 38 cycles) and being unable to perform the qRT-PCR assays in twofold. Doing the qRT-PCR assays in twofold allows to detect abnormal reactions and reduces the noise inherent to qRT-PCR reactions with high $C_t$ levels. Indeed, neurons have a very low copy number of channel mRNA – presumably between 10 and 100 transcripts (Sucher et al., 2000). We therefore decided to pre-amplify the cDNA using an RNA amplification step making it possible to analyze two genes simultaneously with both qRT-PCR assays done in twofold. Working with replicates allowed us to discard assays with a difference higher than 0.5 cycles as these could represent failed qRT-PCR assays or reflect other experimental errors. Averaging the replicates reduced noise and allowed to calculate the errors on the measurements (Pfaffl, 2001). The detection of such problems with the replicates was not possible with a single qRT-PCR assay (Liss et al., 2001) or two assays comparing the relative abundance of 2 transcripts (Aponte et al., 2006). Both qRT-PCR assays for Kv2.1 and GAPD were fully optimized to obtain the highest efficiency but the assay of GAPD nevertheless showed a clear reduction in efficiency with the highest dilution. Therefore, we set a $C_t$ cut-off value of 38 cycles and we strongly recommend setting such limits of detection for qRT-PCR assays. Consequently, such $C_t$ cut-off values makes the correlation with low abundance transcripts not possible without pre-amplification of the mRNA to lower the number of cycles needed. However, it is well documented that this pre-amplification can introduce a bias in the relative abundance between transcripts (Iscove et al., 2002; Ji et al., 2004). Linear amplifications, such as used here, are generally favored compared to exponential ones since the bias tends to be lower (Gustincich et al., 2004; Lockhart and Winzeler, 2000; Nygaard and Hovig, 2006). Because of this phenomenon, transcripts may become over- or under-represented in cells displaying a low expression level compared to cells that have a high expression. This over- or under-estimation would result in an altered slope when correlated with electrophysiological data (Gomes et al., 2003).

Many studies have relied on endpoint PCR (in contrast to qRT-PCR) to obtain a quantitative estimate of the transcript (Geiger et al., 1995; Lambolez et al., 1992). Although both techniques are based on amplification of cDNA, the actual quantification is quite different: qRT-PCR measures the cycles needed to cross a predefined threshold whereas in endpoint PCR the amplified cDNA is measured a posteriori after a fixed number of PCR cycles. Thus, in qRT-PCR an estimation of the amount of transcripts is done at the start of the exponential cDNA amplification whereas in endpoint PCR the estimation is at the end of the reaction. Consequently, the possibility of obtaining the estimate outside the linear range of the PCR amplification is quite high with endpoint PCR especially when as much as 40 cycles are needed when working at the single cell level (Geiger et al., 1995; Lambolez et al., 1992). This makes end-point PCR a noisy technique for quantitative measurements in comparison with qRT-PCR where the estimate is done at the beginning of the linear amplification range. This difference in noise level is obvious in the triplicate reactions on GAPD (Fig. 3A); especially with the 100-fold dilution (reflecting low abundant transcripts) the spread of the triplicate reactions at the predefined threshold (used for quantification in qRT-PCR) is very small compared to the spread above 40 cycles (representing the state of the reaction for estimation in endpoint PCR). Pooling data from multiple cells (Geiger et al., 1995) can reduce this but such pooling does not allow for analysis of cell-to-cell variability, which was our goal.

Single cell expression profiling may become an essential complement to the patch-clamp technique when studying the molecular architecture of ion channels in excitable cells. Despite many molecular studies in heterologous cells, there has been much less emphasis on analyzing the molecular composition of channel protein complexes in native tissue slices or even in vivo. Studying the innate diversity of channel proteins can unveil the function of specific subunits and establish their normal expression levels, which is essential when studying altered expression in disease states.

## Acknowledgments

This work was supported by the 'Fonds voor Wetenschappelijk Onderzoek Vlaanderen' grants FWO-G.0450.03 and FWO-G.0449.11, and a concerted research project Grant BOF-GOA 2004 from the University of Antwerp.

## References

Achard P, De Schutter E. Complex parameter landscape for a complex neuron model. PLoS Comput Biol 2006;2:e94.
Ansel J, Bottin H, Rodriguez-Beltran C, Damon C, Nagarajan M, Fehrmann S, et al. Cell-to-cell stochastic variation in gene expression is a complex genetic trait. PLoS Genet 2008;4:e1000049.
Aponte Y, Lien CC, Reisinger E, Jonas P. Hyperpolarization-activated cation channels in fast-spiking interneurons of rat hippocampus. J Physiol 2006;574:229–43.
Aptowicz CO, Kunkler PE, Kraig RP. Homeostatic plasticity in hippocampal slice cultures involves changes in voltage-gated $Na^+$ channel expression. Brain Res 2004;998:155–63.
Audinat E, Lambolez B, Rossier J. Functional and molecular analysis of glutamate-gated channels by patch-clamp and RT-PCR at the single cell level. Neurochem Int 1996;28:119–36.
Blaine JT, Ribera AB. Heteromultimeric potassium channels formed by members of the Kv2 subfamily. J Neurosci 1998;18:9585–93.
Bochet P, Audinat E, Lambolez B, Crepel F, Rossier J, Iino M, et al. Subunit composition at the single-cell level explains functional properties of a glutamate-gated channel. Neuron 1994;12:383–8.
Bocksteins E, Raes AL, Van de Vijver G, Bruyns T, Van Bogaert PP, Snyders DJ. Kv2.1 and silent Kv subunits underlie the delayed rectifier $K^+$ current in cultured small mouse DRG neurons. Am J Physiol Cell Physiol 2009;296:C1271–8.
Bosch I, Melichar H, Pardee AB. Identification of differentially expressed genes from limited amounts of RNA. Nucleic Acids Res 2000;28:E27.
Bustin SA, Benes V, Garson JA, Hellemans J, Huggett J, Kubista M, et al. The MIQE guidelines: minimum information for publication of quantitative real-time PCR experiments. Clin Chem 2009;55:611–22.
Butler DM, Ono JK, Chang T, McCaman RE, Barish ME. Mouse brain potassium channel beta1 subunit mRNA: cloning and distribution during development. J Neurobiol 1998;34:135–50.
Catterall WA, Goldin AL, Waxman SG. International Union of Pharmacology. XLVII. Nomenclature and structure–function relationships of voltage-gated sodium channels. Pharmacol Rev 2005;57:397–409.
Chandler DP, Wagnon CA, Bolton Jr H. Reverse transcriptase (RT) inhibition of PCR at low concentrations of template and its implications for quantitative RT-PCR. Appl Environ Microbiol 1998;64:669–77.
Chiang LW. Detection of gene expression in single neurons by patch-clamp and single-cell reverse transcriptase polymerase chain reaction. J Chromatogr A 1998;806:209–18.
Clapham DE, Julius D, Montell C, Schultz G. International Union of Pharmacology. XLIX. Nomenclature and structure–function relationships of transient receptor potential channels. Pharmacol Rev 2005;57:427–50.
Derveaux S, Vandesompele J, Hellemans J. How to do successful gene expression analysis using real-time PCR. Methods 2010;50:227–30.
Fitzakerley JL, Star KV, Rinn JL, Elmquist BJ. Expression of Shal potassium channel subunits in the adult and developing cochlear nucleus of the mouse. Hear Res 2000;147:31–45.
Franco D, Demolombe S, Kupershmidt S, Dumaine R, Dominguez JN, Roden D, et al. Divergent expression of delayed rectifier K(+) channel subunits during mouse heart development. Cardiovasc Res 2001;52:65–75.
Gaillard C, Strauss F. Ethanol precipitation of DNA with linear polyacrylamide as carrier. Nucleic Acids Res 1990;18:378.
Geiger JR, Melcher T, Koh DS, Sakmann B, Seeburg PH, Jonas P, et al. Relative abundance of subunit mRNAs determines gating and $Ca^{2+}$ permeability of AMPA receptors in principal neurons and interneurons in rat CNS. Neuron 1995;15:193–204.
Gomes LI, Silva RL, Stolf BS, Cristo EB, Hirata R, Soares FA, et al. Comparative analysis of amplified and nonamplified RNA for hybridization in cDNA microarray. Anal Biochem 2003;321:244–51.
Gustincich S, Contini M, Gariboldi M, Puopolo M, Kadota K, Bono H, et al. Gene discovery in genetically labeled single dopaminergic neurons of the retina. Proc Natl Acad Sci USA 2004;101:5069–74.

Gutman GA, Chandy KG, Grissmer S, Lazdunski M, McKinnon D, Pardo LA, et al. International Union of Pharmacology. LIII. Nomenclature and molecular relationships of voltage-gated potassium channels. Pharmacol Rev 2005;57:473–508.
Hamill OP, Marty A, Neher E, Sakmann B, Sigworth FJ. Improved patch-clamp techniques for high-resolution current recording from cells and cell-free membrane patches. Pflugers Arch 1981;391:85–100.
Hille B. Ion channels of excitable membranes. 3rd ed.; 2001.
Hofmann F, Biel M, Kaupp UB. International Union of Pharmacology. LI. Nomenclature and structure–function relationships of cyclic nucleotide-regulated channels. Pharmacol Rev 2005;57:455–62.
Iscove NN, Barbara M, Gu M, Gibson M, Modi C, Winegarden N. Representation is faithfully preserved in global cDNA amplified exponentially from sub-picogram quantities of mRNA. Nat Biotechnol 2002;20:940–3.
Ji W, Zhou W, Gregg K, Lindpaintner K, Davis S. A method for gene expression analysis by oligonucleotide arrays from minute biological materials. Anal Biochem 2004;331:329–39.
Karrer EE, Lincoln JE, Hogenhout S, Bennett AB, Bostock RM, Martineau B, et al. In situ isolation of mRNA from individual plant cells: creation of cell-specific cDNA libraries. Proc Natl Acad Sci USA 1995;92:3814–8.
Koizumi A, Jakobs TC, Masland RH. Inward rectifying currents stabilize the membrane potential in dendrites of mouse amacrine cells: patch-clamp recordings and single-cell RT-PCR. Mol Vis 2004;10:328–40.
Lambolez B, Audinat E, Bochet P, Crepel F, Rossier J. AMPA receptor subunits expressed by single Purkinje cells. Neuron 1992;9:247–58.
Liss B, Franz O, Sewing S, Bruns R, Neuhoff H, Roeper J. Tuning pacemaker frequency of individual dopaminergic neurons by Kv4.3L and KChip3.1 transcription. EMBO J 2001;20:5715–24.
Lockhart DJ, Winzeler EA. Genomics, gene expression and DNA arrays. Nature 2000;405:827–36.
Mee CJ, Pym EC, Moffat KG, Baines RA. Regulation of neuronal excitability through pumilio-dependent control of a sodium channel gene. J Neurosci 2004;24:8695–703.
Misonou H, Mohapatra DP, Trimmer JS. Kv2.1: a voltage-gated $K^+$ channel critical to dynamic control of neuronal excitability. Neurotoxicology 2005;26:743–52.
Mitarai N, Dodd IB, Crooks MT, Sneppen K. The generation of promoter-mediated transcriptional noise in bacteria. PLoS Comput Biol 2008;4:e1000109.
Moll PR, Duschl J, Richter K. Optimized RNA amplification using T7-RNA-polymerase based in vitro transcription. Anal Biochem 2004;334:164–74.
Nam DK, Lee S, Zhou G, Cao X, Wang C, Clark T, et al. Oligo(dT) primer generates a high frequency of truncated cDNAs through internal poly(A) priming during reverse transcription. Proc Natl Acad Sci USA 2002;99:6152–6.
Nissant A, Lourdel S, Baillet S, Paulais M, Marvao P, Teulon J, et al. Heterogeneous distribution of chloride channels along the distal convoluted tubule probed by single-cell RT-PCR and patch clamp. Am J Physiol Renal Physiol 2004;287:F1233–43.
Nygaard V, Hovig E. Options available for profiling small samples: a review of sample amplification technology when combined with microarray profiling. Nucleic Acids Res 2006;34:996–1014.
Ohya Y, Sperelakis N. Whole-cell voltage clamp and intracellular perfusion technique on single smooth muscle cells. Mol Cell Biochem 1988;80:79–86.
Pfaffl MW. A new mathematical model for relative quantification in real-time RT-PCR. Nucleic Acids Res 2001;29:e45.
Schulz DJ, Goaillard JM, Marder E. Variable channel expression in identified single and electrically coupled neurons in different animals. Nat Neurosci 2006;9:356–62.
Sellner LN, Coelen RJ, Mackenzie JS. Reverse transcriptase inhibits Taq polymerase activity. Nucleic Acids Res 1992;20:1487–90.
Silbert SC, Beacham DW, McCleskey EW. Quantitative single-cell differences in mu-opioid receptor mRNA distinguish myelinated and unmyelinated nociceptors. J Neurosci 2003;23:34–42.
Snyders DJ, Tamkun MM, Bennett PB. A rapidly activating and slowly inactivating potassium channel cloned from human heart. Functional analysis after stable mammalian cell culture expression. J Gen Physiol 1993;101:513–43.
Stahlberg A, Kubista M, Pfaffl M. Comparison of reverse transcriptases in gene expression analysis. Clin Chem 2004;50:1678–80.
Stone BB, Nietupski RM, Breton GL, Weisburg WG. Comparison of Mycobacterium 23S rRNA sequences by high-temperature reverse transcription and PCR. Int J Syst Bacteriol 1995;45:811–9.
Sucher NJ, Deitcher DL, Baro DJ, Warrick RM, Guenther E. Genes and channels: patch/voltage-clamp analysis and single-cell RT-PCR. Cell Tissue Res 2000;302:295–307.
Swain PS, Elowitz MB, Siggia ED. Intrinsic and extrinsic contributions to stochasticity in gene expression. Proc Natl Acad Sci USA 2002;99:12795–800.
Swensen AM, Bean BP. Robustness of burst firing in dissociated purkinje neurons with acute or long-term reductions in sodium conductance. J Neurosci 2005;25:3509–20.
Toledo-Rodriguez M, Blumenfeld B, Wu C, Luo J, Attali B, Goodman P, et al. Correlation maps allow neuronal electrical properties to be predicted from single-cell gene expression profiles in rat neocortex. Cereb Cortex 2004;14:1310–27.
Topal MD, Sinha NK. Products of bacteriophage T4 genes 32 and 45 improve the accuracy of DNA replication in vitro. J Biol Chem 1983;258:12274–9.
Vandesompele J, De Preter K, Pattyn F, Poppe B, Van Roy N, De Paepe A, et al. Accurate normalization of real-time quantitative RT-PCR data by geometric averaging of multiple internal control genes. Genome Biol 2002;3, Research 0034.
Wei AD, Gutman GA, Aldrich R, Chandy KG, Grissmer S, Wulff H. International Union of Pharmacology. LII. Nomenclature and molecular relationships of calcium-activated potassium channels. Pharmacol Rev 2005;57:463–72.
Williams KR, LoPresti MB, Setoguchi M. Primary structure of the bacteriophage T4 DNA helix-destabilizing protein. J Biol Chem 1981;256:1754–62.